SSC-185

The Superconducting Super Collider

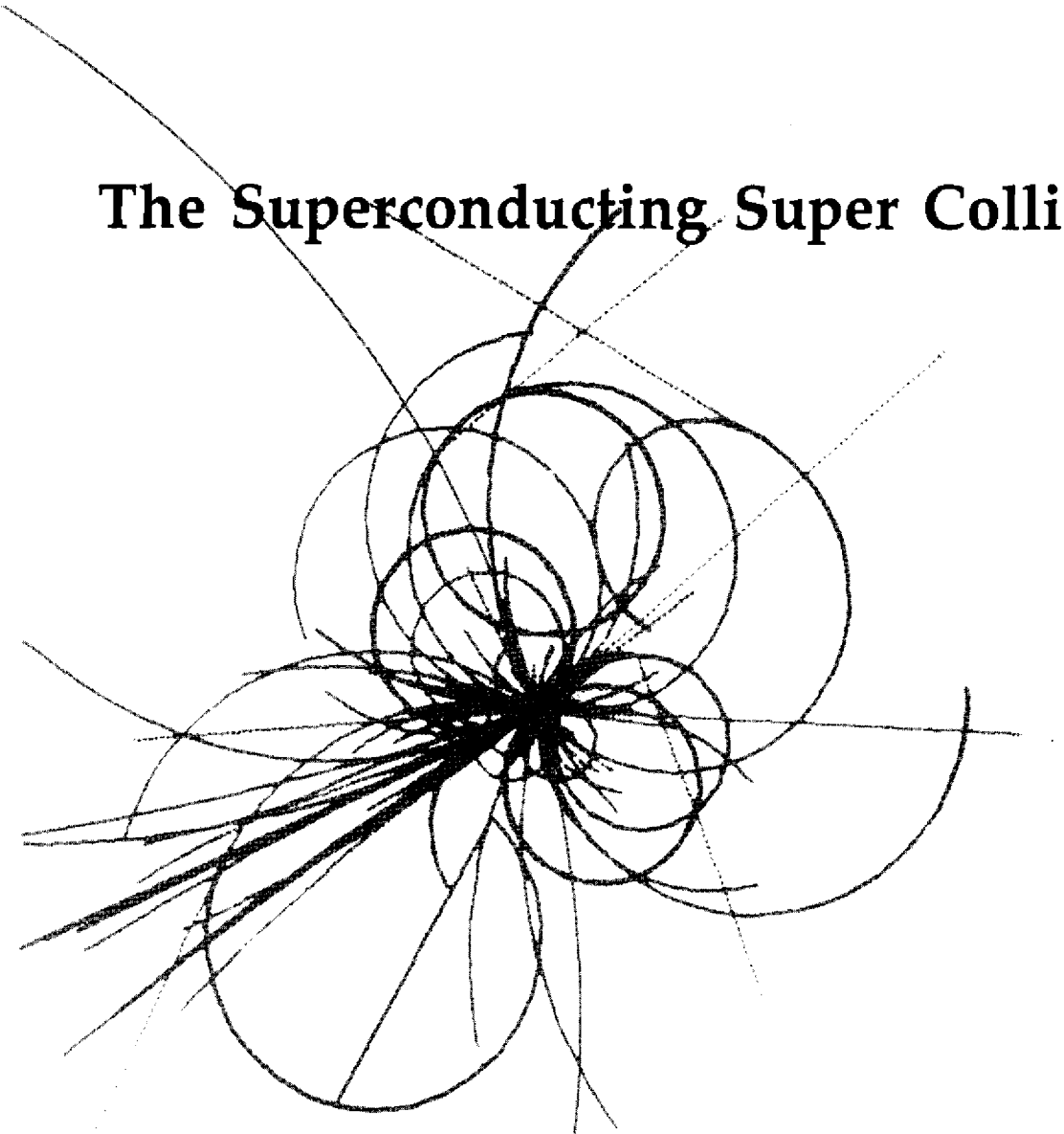

Status of the SSC Superconducting Magnet Program

Presented by John Peoples
for the teams at
BNL, Fermilab, LBL, and the SSC Central Design Group

September 1988

SSC-185

STATUS OF THE SSC SUPERCONDUCTING MAGNET PROGRAM*

Presented by

John Peoples

for the teams at
BNL, Fermilab, LBL, and the SSC Central Design Group†

September 1988

---

* Submitted to the 1988 Applied Superconductivity Conference, San Francisco, CA, September 21–26, 1988.

† Operated by Universities Research Association for the U.S. Department of Energy.

STATUS OF THE SSC SUPERCONDUCTING MAGNET PROGRAM

Presented by

John Peoples

for the teams at
BNL, Fermilab, LBL, and the SSC Central Design Group*
c/o Lawrence Berkeley Laboratory
Mailstop 90-4040
One Cyclotron Road
Berkeley, CA 94720

Introduction

The Superconducting Super Collider (SSC) is a proton-proton collider designed to achieve collisions with 20 TeV per beam, which has been proposed for construction by the U.S. Department of Energy.[1] If our past experience with accelerators is a guide to the future, the knowledge that the SSC will provide will revolutionize the way we think about elementary particles. But before we can have our cake we must bake it. The building of the SSC and its detectors will be a major technological challenge both to the high-energy physics community and to interested industrial firms.

In the SSC, protons are accelerated and stored in two storage rings that are stacked one on top of the other in an underground tunnel 83 km in circumference, large enough to surround Washington, D.C. Collisions can occur at six locations where the proton orbits can be made to intersect. In each collider ring the protons are kept in a roughly elliptical orbit by two types of magnets: dipoles, which bend the proton orbit into a closed loop, and quadrupoles, which deflect the protons back toward the central orbit when they diverge from it. Both types of magnets must use high current density superconducting coils to meet the SSC design requirements. In fact, it is these superconducting coils that make such a supercollider feasible. A dipole field of 6.6 T was chosen as a compromise between the need for the highest practical field and the limits of superconducting technology.[2]

The energy of 20 TeV is somewhat more than twenty times the energy of the highest energy storage ring in operation, the Tevatron, a single-ring proton-antiproton collider at Fermi National Accelerator Laboratory (Fermilab) that was the first synchrotron to use superconducting dipoles. It is still the only superconducting accelerator of this type in operation, although the HERA proton ring at DESY, roughly the size of the Tevatron, is expected to come into operation in 1990.

To illustrate the technological advances that must be made to make the SSC a reality, Table 1 compares the parameters of the SSC with the Tevatron.

Since the dipoles are the most numerous, the most expensive, and, at least traditionally, the most difficult to develop, an R&D program was started in 1984 to develop a dipole meeting all of the systems requirements for the SSC. Some SSC dipole parameters are tabulated in Table 2.

*Operated by the Universities Research Association, Inc., for the U.S. Department of Energy.

Table 1. Selected Tevatron and SSC Parameters.

	Tevatron[3]	SSC
Ring circumference	6.28 km	83.1 km
Operating energy	0.9 TeV (present)	20 TeV (design)
Dipole field strength at operating energy	4 T	6.613 T
Dipole slot length	6.4 m	17.34 m
Number of dipoles	776	7824
Number of quadrupoles	216	1572

Table 2. SSC Collider Ring Dipole Parameters.

Magnetic Properties	
Operating field at 4.35 K	6.613 T
Transfer function* at 1 TeV	1.0309 T/kA
Transfer function at 20 TeV	1.0147 T/kA
Magnetic length**	16.54 m
Linear aperture (diameter)†	21.4 ± 4.0 mm
Critical Mechanical Dimensions	
Slot length‡	17.34 m
Beam tube inner diameter	32.26 mm
Vacuum vessel outer diameter	60.96 cm

†Dipole transfer function is the ratio of the central magnetic field to the current in the coil windings.

**Magnetic length is the integral of the magnetic field with respect to length divided by the central magnetic field.

†Linear aperture is the region within the magnet for which the proton orbits are stable; very roughly speaking, a region in which the field must be uniform to within a few parts in 10^4.

‡Slot length is the physical length that the dipole occupies in each collider ring.

Development of a prototype magnet meeting these parameters has been the goal of a collaboration of Brookhaven National Laboratory, Fermilab, and Lawrence Berkeley Laboratory directed by the Central Design Group (CDG) since the selection of the basic design. During the past year, two full-length prototypes were built, tested, and achieved the design field after fewer than two training quenches, thereby demonstrating that all the parameters could be achieved. Nevertheless, refinement of the dipole continues, as there is clearly room for improvement. Industrial companies have made significant contributions to the dramatic improvements in the performance of superconducting cable during the same period.

Beginning in January 1989, the CDG and the laboratories will provide a selected set of industrial firms with an introduction to the technology and expertise developed in the R&D program. This will be the first phase of a planned three-phase program to enable industrial firms to build the ten thousand superconducting magnets required for the SSC. While the development of the dipole has been a major undertaking on the scale of research and development traditional at the national high-energy laboratories, that effort will be dwarfed by the effort that will be required of industrial firms to fabricate ten thousand magnets meeting the SSC systems requirements.

A cross section of the basic SSC dipole is shown in Figure 1. It consists of a cold mass, a cryostat, and a magnet support system. (Only the first two will be discussed in this paper.) The heart of the cold mass consists of superconducting coils wound from multi-strand superconducting cable. Each strand is made of 6 μ diameter niobium-titanium filaments embedded in a copper matrix. There are four challenges that must be met to build a successful dipole: first, the cable out of which the coils are wound must be capable of carrying the required current; second, the location of the cables must be precisely controlled in the cold mass in order to meet the SSC field quality specifications; third, the coils must be tightly clamped to reduce the inelastic motion of the cable due to magnetic forces to values too low to cause a quench; and fourth, the heat leak into the cryostat must be small enough so that the nearly 8000 dipoles can be cooled down to 4.35 K with a practical refrigeration system. During the past year considerable progress was made in meeting these challenges.

One unique aspect of the SSC is that the proton beam at 20 TeV and full intensity will deposit 2.3 watts of synchroton radiation on the inside of the beam tube of each dipole. The synchrotron radiation heat load is almost a factor of ten larger

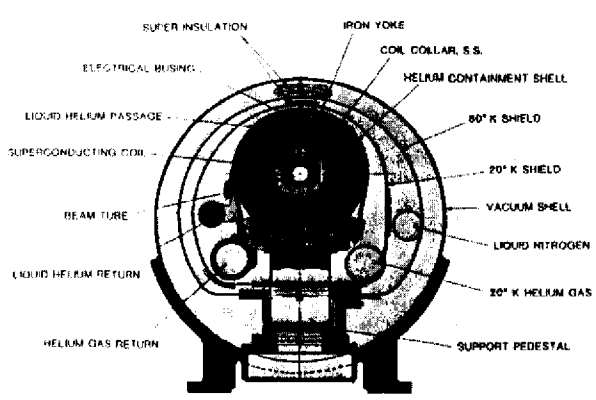

Figure 1. Cross section of the SSC dipole.

than the heat leak budget of the cryostat at 4.35 K. That heat must be conducted away from the beam tube through the iron yoke into the cold helium flow without raising the temperature of the coils more than 50 mK above 4.35 K, the nominal temperature of the cold helium in the magnet.

The work that has been done on the SSC dipole over the past year is summarized in the remainder of the paper, which is divided into four sections: cable development and production, cryostat design, cold mass design, and model magnet testing. (The status of the R&D effort prior to September 1987 may be found in Ref. 4.)

Cable Development and Production

To reach the design field of 6.6 T the average current density in the windings of the inner coil, including the area occupied by insulation and copper, must be 325 A/mm^2. To achieve this high current density the copper-to-superconductor ratio of the inner coil was chosen to be 1.3 to 1. Moreover, the area occupied by the insulation cannot be reduced below its value of roughly 7 percent without compromising the ability of the coils to hold off the large voltages developed during a quench. With the present coil design and copper-to-superconductor ratio, the current density in the superconductor will be 1270 A/mm^2 at 6.6 T. The parameters for the SSC cable are given in Table 3. It should be noted that the design field of 6.6 T refers to the field at the center of the beam tube; the peak field in the magnet, which occurs at the pole turn of the inner coil, is 7 T. The preliminary specifications for the inner-coil cable require that it carry a current of 7167 A in a field of 7 T when the temperature is 4.22 K, corresponding to a current density in the superconductor of 1400 A/mm^2 at 4.35 K.

Table 3. SSC Cable Parameters.

Parameter	Inner Coil	Outer Coil
Wire diameter	0.81 mm	0.65 mm
Copper-to-superconductor ratio	1.3	1.8
Cable midthickness	1.458 mm	1.166 mm
Cable width	9.296 mm	9.728 mm
Cable keystone angle	1.6°	1.2°
Number of strands per cable	23	30
Minimum current at 4.22 K	7167 A at 7 T	7860 A at 5.6 T

The minimum required current density in the superconductor,[4] specified at a field of 5 T and a temperature of 4.22 K, is 2750 A/mm^2. Because there is inevitably some degradation when the wire is made into cable, an allowance of 5 percent has been provided in the cable specification.

Manufacturers have made wire from 12-inch billets that meets this latter specification. Figure 2 shows the performance of wire made by several manufacturers in minimum production lengths of 2200 feet over the past few years. The manufacturers have been making small adjustments to their methods of processing the billets in order to improve their yield. In one instance the current density has fallen below the specification. This is not expected to be a problem, however, as this manufacturer has already demonstrated the ability to meet specifications.

The final parameters of the cable—such as copper-to-superconductor ratio, filament size, and filament spacing—have not been fixed,[5] although we expect to do this in 1989 once the results of the current R&D billet program have been assimilated.

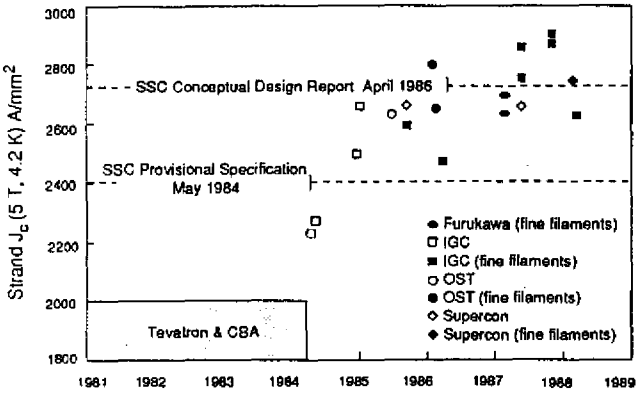

Figure 2. History of J_c of the niobium-titanium superconducting wire for SSC dipole magnets.

A value of J_c exceeding 2750 A/mm^2 would be very desirable: it would allow a copper-to-superconductor ratio higher than 1.3 to 1. Nevertheless, this is not the only critical property of the cable. For example, field quality is very sensitive to random variations in thickness, width, keystone angle, and the compaction of the cable. It is particularly sensitive to errors in conductor location, which in turn are very sensitive to variations in cable thickness and compaction. Since the strand diameter can be controlled quite accurately, variations in cable dimensions are a consequence of cabling. Tolerances for the dimensions of the SSC cable are compared with those for Tevatron and HERA cable in Table 4.

Table 4. Tolerances for SSC, Tevatron, and HERA Cable Dimensions.[6]

Parameter	Tolerances SSC	Tevatron	HERA
Wire diameter	±2.5 μm	±7.6 μm	±10 μm
Midthickness	±6.35 μm*	±12.7 μm	±20 μm
Width	±25.4 μm	±25.4 μm	±30 μm
Keystone angle	±0.1° **	±0.4°	±0.2°

*originally ±12.4 μm
**originally ±0.2°

Control of these dimensions during cabling has noticeably improved. In part this can be attributed to a cabling machine built by LBL that can make both the 23-strand inner cable and the 30-strand outer cable at a maximum rate of 3 m/min.[6] Dimensions of cable produced with this machine can be kept within the tolerances given in Table 4. Recently an improved version of this machine was built for the SSC by an industrial firm.[6] Because it is intended to be a prototype of the cabling machines that will be used to cable the SSC wire, it was designed to cable wire at a rate of 10 m/min. It is anticipated that this machine, once it has been commissioned, will be used by industrial firms to cable wire for prototype SSC dipoles, thus replacing the older machines developed for the Tevatron.

Cryostat Design

An exploded view of the cryostat and cold mass is shown in Figure 3. The cold mass is constrained horizontally and vertically within the vacuum vessel at five locations by four low-friction bearing pads[7]: two in each upper cradle and two in each lower cradle. Each lower cradle is attached to the cold end of a support post. The lower end of the support post is attached to an ambient-temperature plate within the vacuum vessel. Except at the central cradle, the cold mass slides along the bearing surfaces as it shrinks (by 2.9 cm) during cooldown from ambient temperature to 4.35 K. The cold mass is anchored at the center cradle to fix the axial position of the magnet with respect to the vacuum vessel.

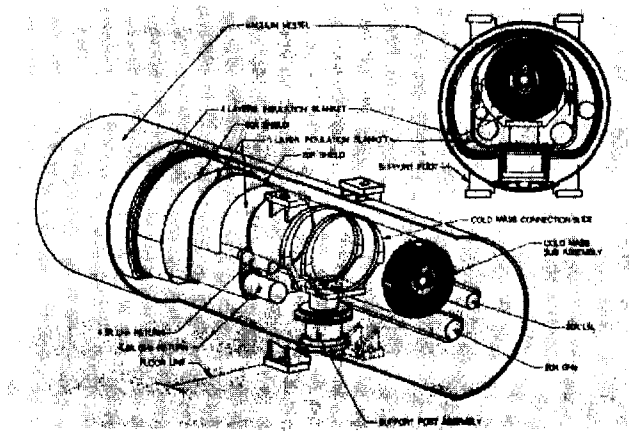

Figure 3. Exploded view of the SSC cryostat and cold mass.

Five support posts were chosen to limit the vertical sag of the cold mass to 0.25 mm.[7] Each support post is a re-entrant column consisting of two tubes. The inner tube is a 127 mm (o.d.) × 3.28 mm (wall) graphite-reinforced epoxy composite. The cold end of this tube is attached to the 4.4 K cold mass; the warm end is connected to an 80 K heat intercept ring and to the outer tube. In addition, there is a 20 K heat intercept ring on the inner tube. The outer tube is a 178 mm (o.d.) × 2.77 mm (wall) fiber-glass-reinforced epoxy composite. The cold end is at 80 K and the warm end is at 300 K. These posts provide a very low heat leak path between the cold mass and the vacuum vessel support rings. Measurements of the heat load for a typical post are given in Table 5.

Table 5. Measured Support Port Heat Loads.[7]

Thermal Station	Heat Load
80 K	1.670 W
20 K	0.414 W
4.5 K	0.020 W

Although the five support posts share the vertical and horizontal loads, the axial load exerted by the cold mass is transferred directly to the center support. The other four supports do not restrain the axial motion of the cold mass because of the low-friction bearings. A single support is not sufficient to withstand the design axial loads, so a method of sharing the axial load among the five supports was developed[7]: the cold ends of pairs of adjacent posts are connected with a tie bar made of a filament-wound graphite-reinforced epoxy

composite tube. Since this composite tube shrinks by only 0.025 mm when cooled to 80 K, the cold ends of the support posts do not change their relative location when the magnet is cooled to 4.5 K, and as a result large bending stresses do not develop in the support columns during cooldown. When the cold mass quenches, the tie bars allow the axial load to be shared among the five columns. The largest axial loads are expected to occur during transportation and installation.

This anchor system has been thoroughly tested in special test fixtures, and recently the complete anchor system was tested in full-length magnet DD0014. Because the DD0014 cryostat was the first of the second-generation design, it was heavily instrumented with strain gauges and thermometers to evaluate the behavior of the support posts and tie bars during cooldown, quenching, and warmup. The stresses in the support posts after cooldown met expectations, and when a quench occurred the axial loads on the posts were shared as expected. Preliminary analysis shows that all of the stresses were well within design limits.

Two thermal shields made of aluminum surround the cold mass and intercept the radiated heat flux. The shields are mounted to the support posts and are connected to the post heat intercept rings by copper cables. One shield is connected to the 80 K intercept and the other is connected to the 20 K intercept. Several multilayer blankets, each consisting of 16 layers of aluminized polyester film and 15 layers of spunbonded polyester, surround the 80 K and 20 K shields. A single blanket is wrapped around the cold mass. The complete assembly is placed inside of a 610 mm (o.d.) vacuum vessel. Measurements of the cryostat heat leak show that it will meet the heat leak budget of 25 W at 80 K, 2.5 W at 20 K, and 0.3 W at 4.35 K. The vacuum vessel is supported externally at two locations.

Cold Mass Design

A cross section of the cold mass is shown in Figure 4. It consists of two sets of inner and outer coils, collar laminations that clamp the coils together, low-carbon steel laminations that form the yoke, multipole correction coils, a beam tube, and a stainless steel skin.

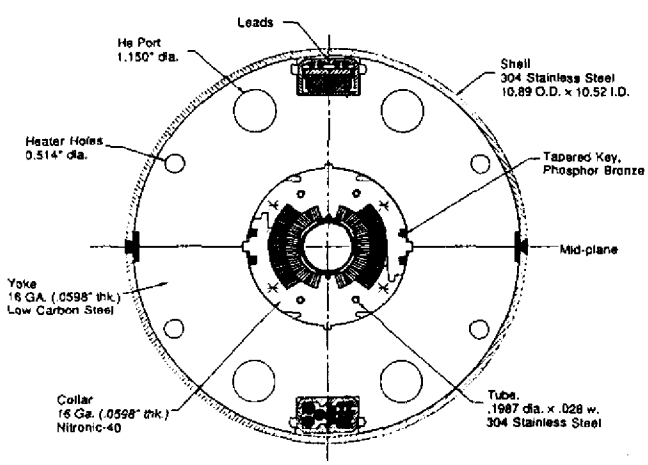

Figure 4. Cross section of the SSC dipole cold mass.

The transverse dimensions of the dipole are set by the inner diameter of the inner coil and by the achievable current density in the coil windings, because these parameters partially determine both the strength of the central field and the size of the field region that meets the field quality specification. As noted earlier, considerations of beam stability determine this region to be an ellipse with a horizontal diameter of roughly 22 mm. The cost of the magnet is proportional to the amount of superconductor used and is therefore roughly proportional to the inner diameter of the inner coil. Given these constraints, and the current densities described earlier, the inner-coil diameter was chosen to be 40 mm.

The inner and outer diameters of the iron yoke also influence the strength of the central field and its uniformity. The transfer function depends on both inner and outer diameters of the yoke. The closer the yoke is to the coil, the greater will be the field for a fixed current in the coils; consequently, less superconductor is needed to achieve the design field. If the yoke is too close to the coils, however, the iron will saturate before the field in the beam tube reaches the design field, causing the good field region to shrink by creating sextupole and decapole fields. If the sextupole and decapole fields generated in this way are not too large, sextupole and decapole coils mounted on the bore tube will compensate for them. Because so little space is available for these windings, the ability to compensate for the deterioration of field quality brought on by saturation is limited. As the iron becomes saturated the transfer function decreases. As noted in Table 1, the transfer function changes by about 1.6 percent as the energy is increased from 1 TeV to 20 TeV. While this latter effect does not necessarily result in a large sextupole or decapole, it does complicate the operation of the storage ring, as discussed in the next paragraph. These two factors led to a choice of 111.4 mm for the inner diameter of the yoke and 276.2 mm for the outer diameter. With this choice the transfer function is 30 percent greater than if an iron yoke were not used.

In addition to the dipoles, which bend the protons into a closed orbit, quadrupoles are needed to provide a restoring force that prevents the protons from drifting into the beam tube walls. Since an ideal quadrupole has a magnetic strength that increases linearly with the distance from the center line, when protons traverse the quadrupole they experience a force proportional to their distance from the quadrupole center line. The magnets of the SSC are organized into cells, each with a horizontally focusing quadrupole and a vertically defocusing quadrupole; between each quadrupole are typically six 17.34-m dipoles. The dipoles and arc quadrupoles (the quadrupoles in the regular cells) suitable for the SSC will have currents in the range of 5 to 10 kA at peak fields. For reasons of economy they were designed to be connected in series to keep to a minimum the number of high-current leads that transport current from ambient temperature to 4.35 K, since the cooling required by the high-current leads is a key factor in determining the size of the refrigeration plant. Since the ratio of focusing strength to bending strength in a ring must remain constant to 5 parts in 10^5 to meet the beam stability criteria,[8] either the ratio of the field gradient of the arc quadrupole to the current must have the same dependence on current as the ratio of central field of the dipole to the current, or there must be a way of correcting for the difference. Since the ratio of the field gradient of the arc quadrupole to the current in its coils decreases by about one-half percent as the energy increases from 1 TeV to 20 TeV, a correction must be made. A trim quadrupole in a cluster of magnets called the correction package—a group of small, separately-powered corrector magnets placed near each arc quadrupole—makes the necessary correction. It has a maximum strength equal to 2 percent of the arc quadrupole, and, because it is a relatively weak magnet, the current leads can be designed for a peak current of 100 A without compromising the corrector design. These trim quadrupoles are connected in series in two circuits corresponding to horizontally focusing and vertically focusing trim quadrupoles to provide the necessary flexibility in adjusting the focusing strength of the lattice. The extra leads do not significantly burden the refrigeration plant.

If a much smaller inner diameter for the dipole yoke had been chosen for the iron—for example, by replacing the non-ferromagnetic collars with iron collars—the amount of

superconductor cable could have been reduced, but the effect of saturation would have been much larger and the correction scheme using low-current trim quadrupoles would not have been feasible. Of equal importance, the sextupole and decapole fields created by saturation of the iron would increase significantly, the scheme for correcting these multipoles would have to be abandoned, and space in the ring would have to be made available for much stronger correctors.

The very large forces that act on the dipole coil when it is excited must also be considered in the design. The separation between the outer edge of the outer coil and the inner edge of the yoke was chosen to be 15 mm to achieve the transfer function. Finite-element calculations done at the time the Conceptual Design Report was written predicted that the largest stainless-steel collar that could be accommodated in this space expanded by 200 μ along the horizontal diameter and contracted by 125 μ along the vertical diameter at a magnet excitation of 6.6 T. On the basis of that prediction, a clearance between the yoke and the stainless-steel collar laminations of at least 300 μ was expected in the first four 17-m magnets designed and constructed by BNL. It was believed that this motion would not cause training if the coils were compressed by the collars at all times during excitation. More detailed calculations done in the past month predict that the collared coil will expand by 320 μ along the horizontal diameter and contract by 270 μ along the vertical diameter.[9] All these magnets exhibited an excessive amount of training, and only one reached the design current.[10] Beginning with the fifth magnet of this design, the yoke was clamped tightly against the collar by inserting shims between the collars and the yokes. The combined yoke-collar structure is now much more rigid than the collar alone, and as a result the coils do not move as much. The fifth full-length magnet, DD0012, reached the design field with no training quenches; the sixth, DD0014, reached the design field after only one training quench.[11] As a result we plan to use the iron yoke as well as the collars to limit the transverse motion of the conductors. Magnets with stainless steel collars that will be built this fall will have redesigned yoke laminations to achieve these objectives without the use of shims.

The development of collared coils is following two paths: the first, which uses stainless steel collars, has already been noted. The second uses aluminum laminations for the collar. From the outset, the aluminum-collared design used the iron yoke to restrain coil motion, because the aluminum collars are not sufficiently rigid.[4] Although these two designs initially had many differences, this is no longer true: a number of the successful features of the aluminum collar have been adapted to the stainless steel collar. In addition to the use of the yoke block to increase the rigidity of the stainless steel collars, both collar designs now use tapered keys to lock the collars together.

To understand the value of tapered keys, consider the collaring process: 150-mm-long packs of collar laminations, each held together by pins, are loosely placed around the four coils. At each longitudinal position there is an upper and lower collar pack. A vertically acting press is used to squeeze the upper and lower collar packs together so that the keys can be inserted. Once inserted, the press is unloaded and the collar packs are locked together. As the press is released, both the collars and coils expand azimuthally until the tensile stress in the collars can resist the expansion of the coils. The nominal cavity created for the coils by the unstressed collars is made smaller than the coils by adding shims at the poles during assembly. In this way, the collars compress the coils even after the press is released. The shims are chosen so that after collaring is completed the collar poles exert a pressure of 8–10 ksi on the inner coils and ~6 ksi on the outer coils. Since the coil shrinks more than the stainless steel collar during cooldown, the pressure decreases to about 5(4) ksi on the inner (outer) coils when the temperature reaches 4.35 K. When the magnet is excited to full field the pressure drops further to about 2 ksi in the inner coils.

The advantage of tapered keys is that they can be partially inserted into the keyways before the coil is completely compressed.[4] At that point the collars are compressed because of the vertical force exerted by the press. Driving the keys into the keyways pulls the collars around the coils and completes the compression of the coil. Prior to using tapered keys it was necessary to oversqueeze the coils by about 5 ksi to get the desired pole pressure on the inner coils after collaring. The oversqueeze caused high local stresses on the Kapton insulation between the turns, particularly at the midplane between the coils where the compressive stresses are largest. Since there is strong evidence from both observation and finite-element calculations for stress gradients across the poles and coil midplane (the surface between the upper and lower coils), local stress concentrations two to three times greater than the average stress may have been encountered, which could have contributed to the insulation failures in early magnets such as DD000Z.

The two types of collar differ significantly in two respects: the stainless steel collars can be spot-welded in pairs at two points, greatly increasing the collar pack rigidity,[12] and the aluminum collars shrink more than the stainless steel collars during cooldown. While it was expected that the aluminum collar would shrink more than the coil and thus increase coil compression after cooldown, that does not appear to be the case. All that can be said is that a coil collared with aluminum appears to lose less prestress than a coil collared with stainless steel. In addition, it appears that a coil collared with aluminum loses more prestress during excitation than a coil collared with stainless steel as a result of the cooldown. That phenomenon is not understood, since the decrease is not consistent with our finite-element models of the coil. There is the possibility that the disagreement is an instrumentation effect: the gauge measures an integral of the stress over the surface of the gauge, which may not be proportional to the average stress. It is likely that there are changes in the stress gradient as well as in the average stress when the coil is either excited or cooled down.

The main thrust of the finite-element calculations and the *in situ* stress measurements is to gain an understanding of the pole stress as a function of current and temperature, since there is strong evidence that, if it is controlled properly, training can either be eliminated or reduced to an acceptable level. Because we believe that both types of collared coils, together with their yokes, can form the heart of a successful dipole, we will continue to develop both types for at least another year or until an obvious choice can be made.

Model Magnet Test Results

The results of model magnet tests prior to October 1987 have already been published[10]; this paper includes only results obtained since then. Five 1-m magnets and one 1.8-m magnet, all built with aluminum collars, have been tested.[12] A tabulation of plateau quench currents at 4.4 K and the number of quenches required to reach the design field are shown in Table 6. Typically, these magnets reached a field within a few percent of the cable short-sample limit after a few training quenches at 4.4 K. Depending on the short-sample limit of the cable, this field is as much as 0.6 T above the design field of 6.6 T. All magnets that were tested at 1.8 K were able to reach or exceed a field of 8.8 T. Typically, the quenches occurred in the outer coil at the high field point just below the short-sample limit. The cause of the quenches is under investigation.

Four 1.8-m magnets with stainless steel collars (the C358 design) and with yokes tightly shimmed against the collars have been built and tested. These magnets reached the short-sample limit of the cable after a few training quenches. A tabulation of the plateau of quench currents achieved at 4.4 K and the number of quenches required to reach the plateau

current is presented in Table 7. At 3.3 K, the lowest temperature that could be reached in the BNL short magnet test apparatus, all but one magnet (DSS10) reached a current consistent with the short-sample limit corresponding to a field greater than 7.5 T. Since the quenches in DSS10 appeared to be in the ramp splice, the electrical connection between the inner and outer coil, it was disassembled. The post-disassembly inspection revealed that the splice had not been properly assembled.

Table 6. Quench Performance of Short Dipoles with Aluminum Collars.

Model Magnet	Initial I_Q at 4.4 K	Training Quenches*	Plateau I_Q at 4.4 K	Maximum I_Q at 1.8 K
D15A3	6212	1	6764	9400
D15A4	6012	1	6820	9278
D15A4F	6238	1	7115	9058
D15A5	5933	1	7084	9400
DSS9†	6050	1	6780	7950‡ (at 3.5 K)
D15A5-R1	5708	3	7000	9386

*Number of training quenches at 4.4 K required to reach or exceed the design field of 6.6 T. Design field is reached at 6550 A with the NC-9 (aluminum collars) design.

†DSS9 is 1.8 m long; all others are 1 m long.

‡Because DSS9 was tested at BNL it could not be tested at 1.8 K.

Table 7. Quench Performance of Short Dipoles with Stainless Steel Collars (C358 Design).

	Initial I_Q at 4.4 K	Plateau I_Q	Temperature	Training Quenches†
DSS6*	6215	6460	4.49 K	5‡
DSS6R	6491	6470	4.50 K	0‡
DSS10**	5416	6510	4.48 K	4‡
DSS11	6372	6690	4.36 K	1‡
DSS12	5895	6730		2‡

*Except in DSS6, the collared coil is restrained by the yoke.

**The ramp splice of DSS10 was damaged during assembly.

†Number of training quenches to reach the plateau current.

‡Cable did not meet SSC specification of 7167 A at 7 T and 4.22 K. Design field of 6.6 T is reached at 6500 A with the C358 design.

Four 17-m dipoles with stainless steel collars and a variety of end restraints have been built and tested in the past year.[11] The first two, DD000Z and DD0010, had "free-standing collared coils" and a weak end restraint. Except for instrumentation these magnets were identically designed. Nevertheless, because small changes in fabrication techniques were being developed while the cold masses were being built, they actually differ slightly. During the testing of DD000Z it was noted that the collared coil underwent an irreversible axial expansion after each quench. Although DD000Z reached 95 percent of the short-sample limit, it took an excessive number of quenches to reach that value. One of its coils was damaged on the thirteenth quench because of an insulation failure, attributed in part to a modification made to the cold mass after it had been completely assembled in an attempt to improve the ends.

Magnet DD0010 reached only 6100 A, barely 90 percent of the cable short-sample limit. While this was a rather disappointing performance, it was not unexpected, since DD0010 was built to the same design as DD000Z. The stress on the pole turn at 5700 A, the largest current for which strain gauge data were obtained, was only 0.6 ksi. At 6100 A it was probably much lower. The magnet was extensively instrumented, and the site of the quench was found to be in the same turn in each quadrant of the inner coil.

Disassembly of magnet DD000Z determined that the collar laminations had bound up against the yoke lamination in an uncontrolled way. As a result it was decided to place shims between the collars and the yokes in DD0012 and DD0014, the third and fourth 17-m dipoles. While these shims were originally intended to limit the axial motion, it was recognized that they would make the combined yoke-collar much more rigid.

Prior to completing DD0012 and DD0014, DSS6 was rebuilt as DSS6R to test the efficacy of this clamping in increasing the azimuthal pressure that the pole exerts on the coils.[13] As noted earlier, DSS6R was very successful. Magnets DD0012 and DD0014 did considerably better than DD000Z and DD0010. Magnet DD0012 reached the design field of 6.6 T, the cable short-sample limit at 4.4 K, on its first excitation and showed no training at 4.4 K. Magnet DD0014 reached the design field of 6.6 T after one quench; after two quenches it reached a plateau of 6.85 T, safely above the design field. Plots of quench current versus quench numbers for these magnets are shown in Figures 5 and 6.

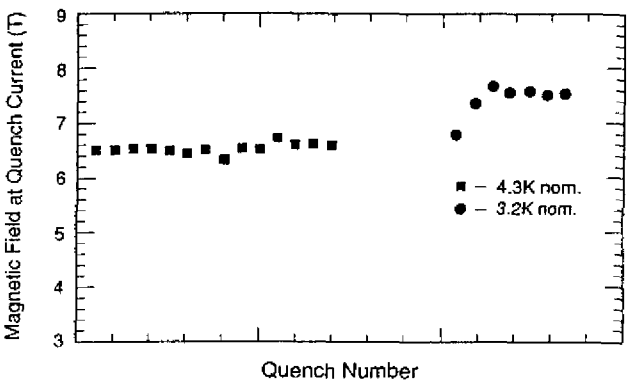

Figure 5. Quench performance of DD0012.

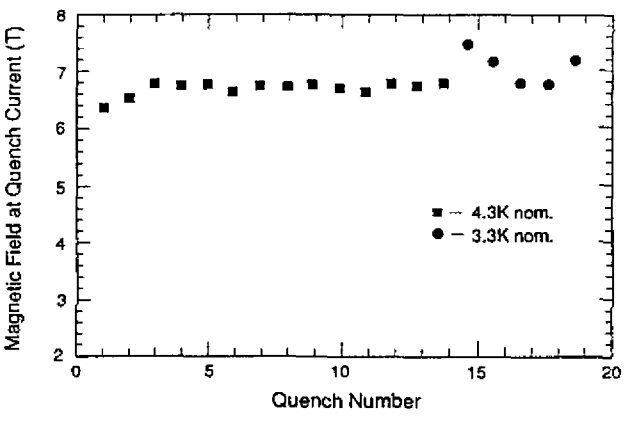

Figure 6. Quench performance of DD0014.

An explanation for the improved performance of DD0012 and DD0014 can be found in a plot of the average azimuthal stress in the inner coil at the pole turn for magnets DD0010, DD0012, and DD0014 shown in Figure 7. At 6400 A this stress was greater than 2 ksi in DD0012 and DD0014; it was only 0.6 ksi at 5700 A in DD0010. We concluded that shimming the yoke laminations against the collar laminations significantly reduced the horizontal expansion and the vertical contraction of the collared coil compared with the situation in DD0010 (and probably in DD000Z) when the magnet was excited to the design field. Since the coil cavity in the collar could not expand as much as it did in earlier magnets, there was less azimuthal and radial motion of the coil, and as a result quenches due to such motion were virtually eliminated.

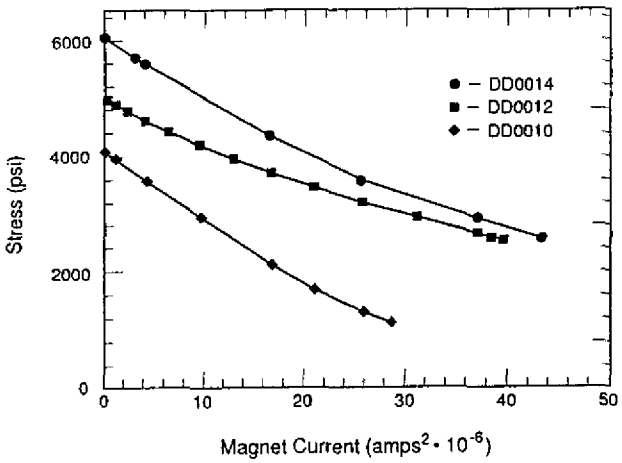

Figure 7. Azimuthal coil stress as a function of current in 17-m magnets.

Three more 17-m magnets were built in the past year and await testing. Two, DD0011 and DD0013, were collared with aluminum.

The low value of azimuthal coil stress at the pole turn in DD0010 can be attributed not only to the failure of the collars to limit the azimuthal and radial motion of the coil, but also in part to large variations in the azimuthal circumference of the coil cross section. While it had been intended to control these dimensions to within 50 μ, we have found that after curing the coils there is a systematic variation of this dimension along the length of the coil of roughly 200 μ. Since it is systematic, and since the same curing press and form blocks are used to cure the upper and lower coils, a large systematic variation in the azimuthal coil stress along the length of the collared coil is caused by the variation in coil dimensions. Although it was recognized more than a year ago that this was caused by the curing fixtures, new fixtures that will hold the coil circumference to the desired 50 μ will not be available until early in 1989. In the meantime, we believe that the existing fixtures have been sufficiently improved to limit variations in the azimuthal coil circumference to 100 μ.

Because of the many improvements to all coil and collaring fixtures, we expect that dipoles made starting this fall will either meet or exceed the performance of DD0012 and DD0014. We certainly expect them to reach the design field without excessive training.

Although DD0012 and DD0014 reached fields as high as 7.6 T when operated at 3.3 K, it was not possible to excite them to the cable short-sample limit because of quenches in the ramp splice. All quenches at 3.3 K in DD0014 and nearly all quenches in DD0012 at 3.3 K and 2.5 K were initiated in the vicinity of the ramp splice. We are confident that the ramp splice was the cause of the quenches; the quench sites were located with signals from voltage taps attached to the coils. Because it is difficult to support the ramp splice along its roughly 30 cm length, it is not surprising that quenches occur there due to cable motion. This difficulty was first recognized in DSS10, a 1.8-m dipole tested at BNL. A newly-designed ramp splice design, which gives the cable much better mechanical support throughout the transition region, will be tested in a 1.8-m magnet in the near future. Once the new ramp splice has been successfully developed it will be incorporated into future 17-m magnets of this design. In addition, magnets DD0010, DD0012, and DD0014 will be rebuilt (using the original coils) with the improved ramp splice, a common type of collar, and a common end restraint.

Summary

We expect to build and test sufficient magnets in 1989 to enable us to choose the final dipole cross section, a crucial step toward industrial manufacture of the dipoles.

Acknowledgements

I thank Valerie Kelly and Donna Matthews for their conscientious attention to detail in preparing this paper for publication. I thank Kate Metropolis for the considerable help that she provided me while editing the text.

References

[1] J. D. Jackson, ed., Conceptual Design of the Superconducting Super Collider, SSC-SR-1020, March 1986, p. 3.
[2] Ibid., p. 267.
[3] H. T. Edwards, Ann. Rev. Nucl. Sci. 35, 605 (1986).
[4] C. Taylor, "SSC Magnet Technology," presented at the 10th International Magnet Technology Conference, Boston, MA, 1987 and Lawrence Berkeley Laboratory Report LBL-23123.
[5] R. Scanlan, J. Royet and R. Hannaford, "Evaluation of Various Fabrication of Fine Filament NbTi Superconductors," in IEEE Trans. on Magnetics MAG-23, March 1987, p. 1719.
[6] R. Scanlan, J. Royet and R. Hannaford, "Fabrication of Rutherford-Type Superconducting Cables for Construction of Dipole Magnets," in ICMC Conference on Cryogenic Materials Applications and Properties, Shenyang, P. R. China, June 1988, and Lawrence Berkeley Laboratory Report LBL-24321.
[7] R. C. Niemann et al., "Second Generation Superconducting Super Collider Dipole Magnet Cryostat Design," presented to this conference LF-3.
[8] J. D. Jackson, ed., Conceptual Design of the Superconducting Super Collider, SSC-SR-1020, March 1986. As revised September 6, 1988.
[9] C. Goodzeit and M. Rehak, "Analysis of Collars for SSC," SSC-MD-202 [also BNL-291-15] (July 25, 1988).
[10] J. Strait et al., "Test of Prototype SSC Magnets," Presented at the 10th International Conference on Magnet Technology (MT-10), Boston, MA (September 1987), and Fermi National Accelerator Laboratory Report TM-1479.
[11] J. Strait et al., "Tests of Full Scale SSC R&D Dipole Magnets," presented at the 1988 Applied Superconducting Conference (LA-3), San Francisco, CA (August 1988).
[12] W. S. Gilbert et al., "Magnetic Field Decay in Model SSC Dipoles," presented at the 1988 Applied Superconducting Conference (LA-5), San Francisco, CA (August 1988).
[13] P. Wander et al., Test Results from 1.8 m SSC Model Dipoles, presented at the 1988 Applied Superconducting Conference (LA-2), San Francisco, CA (August 1988).